The Active Site Cysteine of Ubiquitin-Conjugating Enzymes Has a Significantly Elevated pK_a: Functional Implications†

Blanton S. Tolbert,‡ Stephen G. Tajc,‡,§ Helen Webb,§,|| Jessica Snyder,‡ Jens E. Nielsen,|| Benjamin L. Miller,‡,⊥ and Ravi Basavappa*,‡

Department of Biochemistry and Biophysics, University of Rochester School of Medicine and Dentistry, Rochester, New York 14642, Department of Biochemistry, Conway Institute, University College Dublin, Belfield Dublin 4, Ireland, and Department of Dermatology, University of Rochester School of Medicine and Dentistry, Rochester, New York 14642

Received July 22, 2005; Revised Manuscript Received October 18, 2005

ABSTRACT: Ubiquitin-conjugating enzymes (E2s or Ubcs) are essential components in the ubiquitination apparatus. These enzymes accept ubiquitin from an E1 enzyme and then, usually with the aid of an E3 enzyme, donate the ubiquitin to the target protein. The function of E2 relies critically on the chemistry of its active site cysteine residue since this residue must form a thioester bond with the carboxyl terminus of ubiquitin. Despite the plethora of structural information that is available, there has been a notable dearth of information regarding the chemical basis of E2 function. Toward filling this large void in our understanding of E2 function, we have examined the pK_a of the active site cysteine using a combination of experimental and theoretical approaches. We find, remarkably, that the pK_a of the active site cysteine residue is elevated by approximately 2 pH units above that of a free cysteine. We have identified residues that contribute to the increase in this pK_a. On the basis of experimental values obtained with three different E2 proteins, we believe this to be a general and important characteristic of E2 protein chemistry. Sequence comparison suggests that the electrostatic environment is maintained not through strict residue conservation but through different combinations of residues near the active site. We propose that the elevated pK_a is a regulatory mechanism that prevents the highly exposed cysteine residue in free E2 from reacting promiscuously with electron deficient chemical moieties in the cell.

The covalent attachment of ubiquitin to proteins is used to regulate a myriad of basic cellular processes, such as the cell division cycle, gene expression, DNA repair, endocytosis, and general protein turnover (*1*, *2*). Despite the many effects of ubiquitin modification, each is initiated by the same set of three enzymatic activities: E1 (ubiquitin-activating enzyme), E2 (ubiquitin-conjugating enzyme), and E3 (ubiquitin ligase). The reaction scheme commences with E1, which activates ubiquitin by forming a thioester bond between its catalytic cysteine and the C-terminal carboxyl group of ubiquitin. E2 then accepts ubiquitin from E1 to form a thioester bond between the E2 catalytic cysteine residue and the ubiquitin C-terminus. E2, usually in concert with a cognate E3, then donates the ubiquitin to a lysine residue of the target protein. Polyubiquitination of the target protein typically leads to recognition and destruction by the proteasome, whereas monoubiquitination has diverse consequences.

As a reflection of the stringent structural requirements for E2 function, every known E2 structure has the same core fold (the "UBC fold"), which consists of an $\alpha+\beta$ arrangement and a 3_{10}-helix. Structural variations of the UBC fold occur, but are localized primarily to the extremities of the molecule. The current model of E2 function proposes that specificity for different E3s or substrate proteins is conferred at these extremities while the core fold has been conserved to allow recognition of the common factors of the pathway, namely, E1 and ubiquitin.

The active site cysteine is located in the core UBC fold. It is positioned at the N-terminus of a 3_{10}-helix, and surrounded mainly by an adjacent α-helix and two loop segments. In this context, the cysteine is placed at the base of a shallow groove on the surface of the protein, and is circumscribed by conserved residues of the UBC family. The important question of how the chemistry of the active site is modulated to render catalytic competence arises. Remarkably, very little still is known about the active site chemistry. A recent study has shown that a conserved asparagine residue (part of the strictly conserved HPN motif) is critical for the transfer of ubiquitin to the target protein (*3*). The asparagine may stabilize the negative charge of the oxyanion formed during lysine attack by the substrate protein. Even less is known about the transfer of ubiquitin to E2 from E1. The transfer step necessitates deprotonation of the catalytic cysteine to form the nucleophilic thiolate intermediate on

† This work was funded in part by NIH Research Grants R01-GM-57536 (to R.B.) and R01-GM-62825 (to B.L.M.), a Leukemia and Lymphoma Society Scholar Award (to R.B.), and NIH Training Grant T32AR007472 (for S.G.T.).

* To whom correspondence should be addressed. E-mail: Ravi_Basavappa@urmc.rochester.edu.

‡ Department of Biochemistry and Biophysics, University of Rochester School of Medicine and Dentistry.

§ These authors contributed equally to this research.

|| University College Dublin.

⊥ Department of Dermatology, University of Rochester School of Medicine and Dentistry.

10.1021/bi0514459 CCC: $30.25
Published on Web 11/22/2005

E2. Deprotonation is a function of the pK_a for the cysteine and can be altered depending on its local environment.

To understand the chemistry of the catalytic cysteine, we have measured its pK_a experimentally. We demonstrate that the pK_a of the catalytic cysteine is shifted approximately 2 pK_a units above that of a model cysteine in solution (pK_a ~ 8.5). Using structure-based pK_a calculations (based on the finite difference Poisson−Boltzmann equation), we further show that this is a conserved property of the E2s engendered at the level of their secondary and tertiary structures. This intriguing result indicates that the active site cysteine is much less reactive than a free cysteine. We suggest that this represents a control mechanism that prevents promiscuous reactivity of the E2s with random electron poor molecules (electrophiles) in the cell. As a result, a constant pool of competent E2s will be available in the cell.

MATERIALS AND METHODS

DNA Constructs and Protein Preparation. The preparation of wild-type and mutant (C114S) UbcH10[1] constructs (pET 28 expression vector) has been described elsewhere (*4*). UbcH10 C102S and the double mutant C102S/C114S were prepared by site-directed mutagenesis following the Stratagene Quick Change protocol. All mutations were confirmed by sequencing. The cDNA for both Ubc2 and Ubc13 were purchased from Open Biosystems. The genes were cloned using the LIC protocol (*5*) into a vector encoding an N-terminal six-His tag (generously provided by E. Phyzicky and B. Grayhack, Department of Biochemistry and Biophysics, University of Rochester School of Medicine and Dentistry).

All proteins were expressed in BL21(DE3) RIL cells using conventional IPTG-based expression procedures. Cells were lysed by a combination of lysozyme treatment and tip sonication. Each E2 was purified by nickel affinity chromatography on Hi Trap columns (Amersham Biosciences), and protein homogeneity (>95%) was confirmed by SDS−PAGE (Coomassie staining).

Determination of pK_a by A_{240}. UV measurements were performed on a Spectronic Genesys 2 spectrophotometer at room temperature. All E2 concentrations were 10−15 μM. For pK_a determination, the proteins were prepared in a triple buffer system (containing 30.0 mM AMPSO, 30.0 mM NaP, and 30.0 mM NaPP) covering a pH range of 6−12 (*6*). All A_{240} signals were collected in the linear range of the instrument (0.05−1.0) using buffer only solutions to correct for background absorption and/or scattering.

pK_a As Determined by ITC. ITC experiments were performed on a Microcal VP isothermal titration calorimeter (Microcal, Northampton, MA) as previously described (*7*), with the following modifications. The E2s were buffer exchanged into a triple buffer (30.0 mM AMPSO, 30.0 mM NaP, and 30.0 mM NaPP) system at the desired pH using a Bio-Rad Econo-Pac 10DG desalting column. The final E2 concentrations (50−150 μM) were determined by the Bradford assay and using the appropriate A_{280} molar extinction coefficients. For the pK_a determination, a single 2.0 μL injection of degassed iodoacetamide (50−150 mM) was performed at 30 °C, with stirring at 290 rpm. The reaction was allowed to proceed until the power signal returned to baseline. The reaction was determined to be complete by allowing four additional injections of iodoacetamide into the cell and observing endothermic thermograms, which were identical to buffer only controls. Data were analyzed as previously described (*7*).

Preparation of the PDB Files for pK_a Calculations. 1JBB (ubiquitin-conjugating enzyme Ubc13, from *Saccharomyces cerevisiae*), 1I7K (ubiquitin-conjugating enzyme UbcH10, from *Homo sapiens*), and 1JAS (ubiquitin-conjugating enzyme Ubc2, from *H. sapiens*) were downloaded from the Protein Data Bank (*8*). The PDB files were regularized using WHAT IF (*9*). All crystallographic water molecules were eliminated from the PDB files, and all missing protein atoms were rebuilt using WHAT IF. pK_a calculations were performed on model 1; the first protein chain in the PDB file and only the dominant rotamer conformations were used.

pK_a Calculations. pK_a calculations were performed using the WHAT IF pK_a calculation routines as described previously (*10*), with the exception that a uniform protein dielectric constant was used. Hydrogen atoms were added to the models using the algorithms within WHAT IF. The positions of these hydrogen atoms were refined by optimizing the global hydrogen bond network. We used the Poisson−Bolztmann equation (PBE) solver DelPhi II (*11*) to obtain electrostatic energies. The following PBE parameters were used: number of focusing runs, 4; final PBE map resolution, 0.25 Å/grid point; protein dielectric constant, 8; solvent dielectric constant, 80; ionic strength, 144 mM; ionic exclusion radius, 2.0 Å; and solvent probe radius, 1.4 Å. Titratable groups included in the pK_a calculations were the N-terminus, Asp, Cys, Glu, His, Lys, Arg, Tyr, and the C-terminus. Only the transition from neutral to positively charged was included for histidine residues.

Decomposition of pK_a Values. pK_a values of residues in the folded protein are most commonly compared to so-called "model compound" pK_a values. These model compounds mimic the chemical properties of amino acid side chains and serve as a reference state for the pK_a value of an amino acid side chain isolated in solution. We calculated pK_a values in the folded protein by computing the change in the environment of the amino acid side chain when transferred from solution to its position in the protein (*10*, *12*). We thus calculated ΔpK_a values that arise from effects of the protein environment. The ΔpK_a values are generally computed as a sum of three terms: the desolvation effect, the interaction with permanent charges and dipoles (the background interaction energy), and the interaction with other titratable groups. Generally, the immediate environment of a titratable group determines the desolvation effect and the background interaction energy, whereas the interaction with other titratable groups often is determined by groups at varying distances. To identify the residues with titratable groups that influence the pK_a of the active site cysteine residue, we calculated in a pairwise fashion the change in the pK_a of the cysteine thiol due to interaction with each of the other titratable groups. Briefly, for a protein consisting of a number N of titratable groups, denoted (T_1, T_2, T_3, ..., T_N) and for which the pK_a value of group T_i in the folded protein due to interactions with other titratable groups is denoted $\Delta pK_{aElec,T_i}$(all), we calculate the effect of group T_j on T_i by calculating

[1] Abbreviations: Ubc, ubiquitin-conjugating enzyme; ITC, isothermal titration calorimetry.

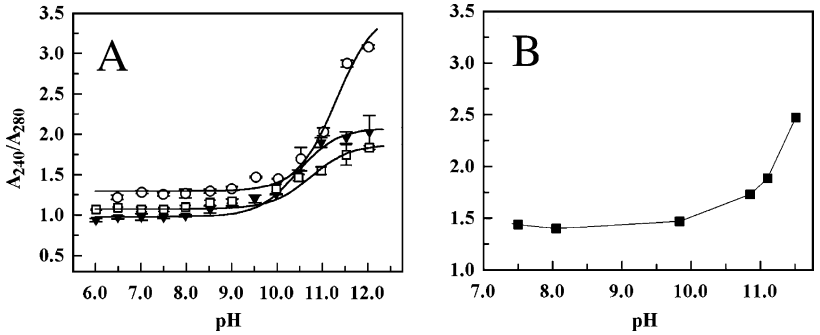

FIGURE 1: Experimental A_{240} titration results. (A) UbcH10 C102S (○), Ubc2 (▼), and Ubc13 (□). The dark lines represent fits of the experimental data to the Henderson−Hassellbach equation. (B) A_{240} control titration on UbcH10 C102S/C114S.

the ΔpK_a values for T_j and T_i in a system that contains only these two groups. We thus arrive at a new ΔpK_a value for T_i denoted $\Delta pK_{aElec,T_i}(T_j)$, where the ΔpK_a value of T_i is influenced by only T_j. The ΔpK_a values for T_i and T_j are calculated by evaluating the Boltzmann sum at every $^1/_{10}$ of a pH value from pH 2.0 to 14.0. We can thus calculate $\sum_{j=1}^{N} \Delta pK_{aElec,T_i}(T_j)$, and if the system behaves ideally (i.e., all effects are additive), then $\sum_{j=1}^{N} \Delta pK_{aElec,T_i}(T_j) = \Delta pK_{aElec,T_i}$(all). For many systems, this last relation does not hold due to the inherent nonadditivity of strongly coupled systems of titratable groups. However, in the case of E2 proteins, additivity seems to hold on the basis of the agreement of calculated and experimental pK_a values.

RESULTS AND DISCUSSION

E2 Active Site pK_a Measurement by UV Absorbance. The ionization of cysteine thiol to thiolate can be monitored quantitatively by measuring the absorbance signal of the latter species at 240 nm (*13*−*16*). This method has been utilized to establish the pK_a of the catalytic cysteine residues for a number of proteins, including those of the thioredoxin superfamily (*13*−*16*). In our study, we used the A_{240} method to measure the apparent pK_a of three E2 proteins: UbcH10 (*H. sapiens*), Ubc2 (*S. cerevisiae*), and Ubc13 (*S. cerevisiae*). It should be noted that Ubc2 and Ubc13 contain only the catalytic cysteine residue, whereas UbcH10 has a second, buried cysteine residue (C102). Unless otherwise stated, all experiments with UbcH10 were performed with a mutant of UbcH10 in which cysteine 102 was changed to a serine.

The influence of pH on the absorbance signal at 240 nm was measured for each E2 in triplicate at 25 °C. The results are summarized in Figure 1. It was necessary to normalize the absorbance signal at 240 nm to 280 nm. This correction was made because the protein molar extinction coefficient at 280 nm is pH sensitive. As shown in Figure 1A, all three E2s exhibit the classic Henderson−Hasselbach titration profile indicative of a weak acid titration. Very surprisingly, the midpoints of all titration curves are shifted well above that for a model cysteine, which has a pK_a of ∼8.5, suggesting a significantly elevated pK_a.

To unequivocally assign the titration to that of the catalytic cysteine, we cloned a cysteine-less mutant of UbcH10 (UbcH10 C102S/C114S) and repeated the titration. The results are summarized in Figure 1B. UbcH10 C102S/C114S exhibited a titration curve identical to that of UbcH10 C102S. Thus, while these preliminary titrations clearly indicate that the active site cysteine does not behave like free cysteine, our ability to arrive at a precise pK_a value is compromised by the presence of other ionizable species. In most other reports using the A_{240} method, the pK_a was found to be shifted 2−4 pH units below 8.5. However, Holmgren et al. (*13*) have shown that tyrosine ionization complicates the ability of the A_{240} approach to unambiguously monitor an elevated level of cysteine deprotonation. Thus, though the A_{240} method can be used to determine values of pK_a shifts when the shift is toward the acidic region, it can only indicate that the pK_a is elevated but cannot give a reliable value when the shift is toward the more alkaline region.

E2 Active Site pK_a Measurement by Isothermal Titration Calorimetry. To circumvent the limitations of the A_{240} method, we used isothermal titration calorimetry to specifically follow the ionization state of the cysteine thiol as a function of pH (*7*). In short, this method relies on monitoring the initial rate of the reaction of the thiolate anion with iodoacetamide (a thiolate specific probe). Due to the laws of mass action, as the concentration of thiolate (which is a function of pH) increases, so will the initial rate of the chemical reaction. Thus, one can quantitate the formation of thiolate at various pH values by monitoring the initial rate of the reaction with iodoacetamide. By plotting the maximum ITC response signal $(dq/dt)_{max}$ (which is proportional to the intial rate of reaction in a kinetic application of ITC) versus pH, one obtains a Henderson−Hassellbach titration profile (*7*). The results of the E2 experiments are summarized in Figure 2A and Table 1. In agreement with the A_{240} results, the ITC results indicate elevated pK_a values for all three E2 proteins. More specifically, each E2 protein shows a shift in the pK_a value of its active site cysteine of approximately 2 pH units above that for a model cysteine. Importantly, no reactivity of iodoacetamide with the cysteine-less mutant is observed (Figure 2B), and control experiments verified that iodoacetamide does not react with free tyrosine (data not shown). Thus, the ITC method is reporting only the ionization state of the cysteine residue, as desired.

The structures of all three E2 proteins have been determined to high resolution, and each shows that the catalytic cysteine residues are surface-exposed with their side chains solvent accessible (*4*, *17*, *18*). The presence of a pK_a shifted as high as 10.5 for a solvent accessible group is intriguing. One would expect that a surface-exposed cysteine would have properties similar to those of a model cysteine, due to its close contact with the surrounding solvent. Instead, all three E2 proteins have an elevated pK_a for their active site cysteine. Because the active site cysteine is located toward the N-terminal end with respect to a strictly conserved 3_{10}-helix, one might hypothesize that the altered pK_a could be

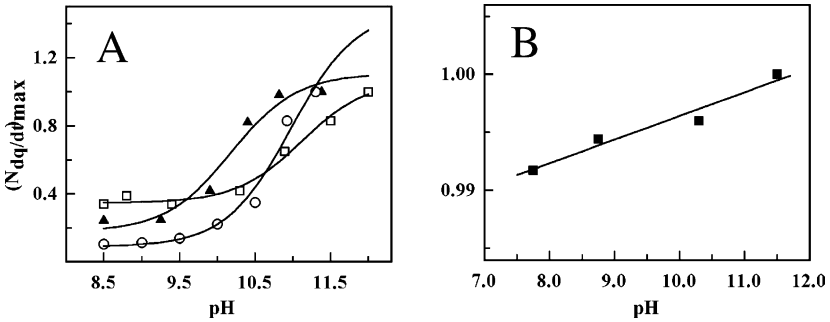

FIGURE 2: pK_a measurement by ITC. (A) UbcH10 (○), Ubc2 (▲), and Ubc13 (□). The dark lines represent fits of the experimental data to the Henderson−Hassellbach equation (*7*). The values on the *y*-axis are normalized to $(dq/dt)_{max}$ at the highest pH value for each E2. (B) UbcH10 C102S/C114S ITC control titration.

Table 1: Summary of Measured and Calculated pK_a Values for UbcH10, Ubc2, and Ubc13

E2 (PDB entry)	exp pK_a (ITC)[a]	calc pK_a[b]	ΔpK_a (exp − calcd)[c]	ΔpK_a (exp − model)[d]
UbcH10 (1I7K)	10.9 ± 0.2	10.49 ± 0.75	0.41	2.4
Ubc2 (1JAS)	10.2 ± 0.2	10.44 ± 0.75	−0.24	1.7
Ubc13 (1JBB)	11.1 ± 0.1	11.27 ± 0.75	−0.17	2.6

[a] The experimental value of the active site cysteine pK_a as measured by ITC for each protein. [b] The calculated value of the active site cysteine pK_a for each E2 protein. [c] The difference in pK_a values determined by experiment and by calculation. [d] The difference in pK_a values for the active site cysteine and free cysteine.

due in part to the effect of the helix dipole moment. However, our observation of an elevated pK_a for each Ubc is in stark contrast to the work of Creighton and co-workers (*15*), who demonstrated that the cysteines located toward the N-terminal end with respect to a set of test α-helical peptides displayed pK_a values lowered by 1.6 pK units. Thus, the highly shifted pK_a values for the Ubcs determined herein must originate from the spatial positioning of charged groups in the vicinity of the active site. We attempted to study the basis for the elevated pK_a by undertaking an analysis of the active cysteine pK_a in UbcH10 mutants in which putatively influential residues were mutated to Ala. Unfortunately, these mutants were expressed too poorly for analysis by ITC, which suggests that the target residues are important for folding stability and/or function.

E2 Active Site pK_a Calculations. Since we could not decompose the contributions of the nearby residues using appropriate mutant proteins, we instead used a computational approach. pK_a calculations were carried out as described in Materials and Methods to dissect the effects that elevate the pK_a value of the active site cysteine. To check the accuracy of the computational method, we calculated the pK_a values of the catalytic cysteine residues of the wild-type proteins and compared them to our experimental values. The results of the pK_a calculations on Ubc13 (PDB entry 1JBB), UbcH10 (PDB entry 1I7K), and Ubc2 (PDB entry IJAS) are summarized in Table 1. These results reveal excellent agreement between the experimental and computational methods and provided us with confidence to proceed with the computational decomposition of the pK_a values.

Decomposed pK_a Values. To understand the origins of the highly elevated pK_a values of the active site cysteines in this study, it is instructional to decompose the pK_a value shifts into effects originating from the nontitratable and titratable part of the protein. The pK_a of a residue is dependent on the free energy difference between the neutral and charged forms of the residue in a protein. This free energy difference between the neutral and charged states of the residue is influenced both by its nontitratable environment and by the other titratable groups in the protein. The effect of the nontitratable environment consists of the desolvation energy and the background interaction energy. The desolvation energy describes the costs of moving the neutral and charged forms of a group from water to its position in the protein, whereas the background interaction energy describes the difference in the interaction energy between the charged form and the neutral form of each titratable group, with the permanent dipoles and charges of the protein. Both the desolvation and background interaction energies usually are assumed to be pH-independent quantities, and are influenced primarily by the immediate environment of the titratable group. The effect of the titratable environment on a pK_a value is strongly pH-dependent and typically originates from a larger set of residues. The effect of the titratable environment can be decomposed further into the effect of individual titratable groups.

Decomposition of pK_a values for the active site cysteine residues in Ubc13 (PDB entry 1JBB), UbcH10 (PDB entry 1I7K), and Ubc2 (PDB entry 1JAS) were performed as described in Materials and Methods. The total effects due to the titratable groups and the nontitratable groups are shown in Figure 3A. The pK_a value for the buried residue Cys102 in UbcH10 cannot be decomposed since the calculations predict an extremely high pK_a value for this residue. The effects of the six most influential titratable groups on the pK_a of the catalytic cysteine of each E2 also are given in Figure 3A. The spatial dispositions of these important residues are shown in Figure 3B for UbcH10. Four of the six residues are acidic residues, namely, aspartic and glutamic acid residues. The other two residues are lysines. The model shows the placement of the residues around the active site. As is evident from the model, the acidic residues surround the catalytic cysteine. In this context, these residues can act as a charge antagonist by preventing the deprotonation of the catalytic cysteine residue, and hence elevate its pK_a. Only one of the lysine residues has its side chain pointed toward the cysteine residue. If just the charges of the six residues are taken into account, a net of two negative charges are in the proximity of the active site, and are sufficient to suppress the deprotonation of the cysteine.

Conservation of the Elevated pK_a. The uniformly high pK_a values for all three E2 proteins that were tested suggest that the elevated pK_a may be a common feature of all E2 proteins.

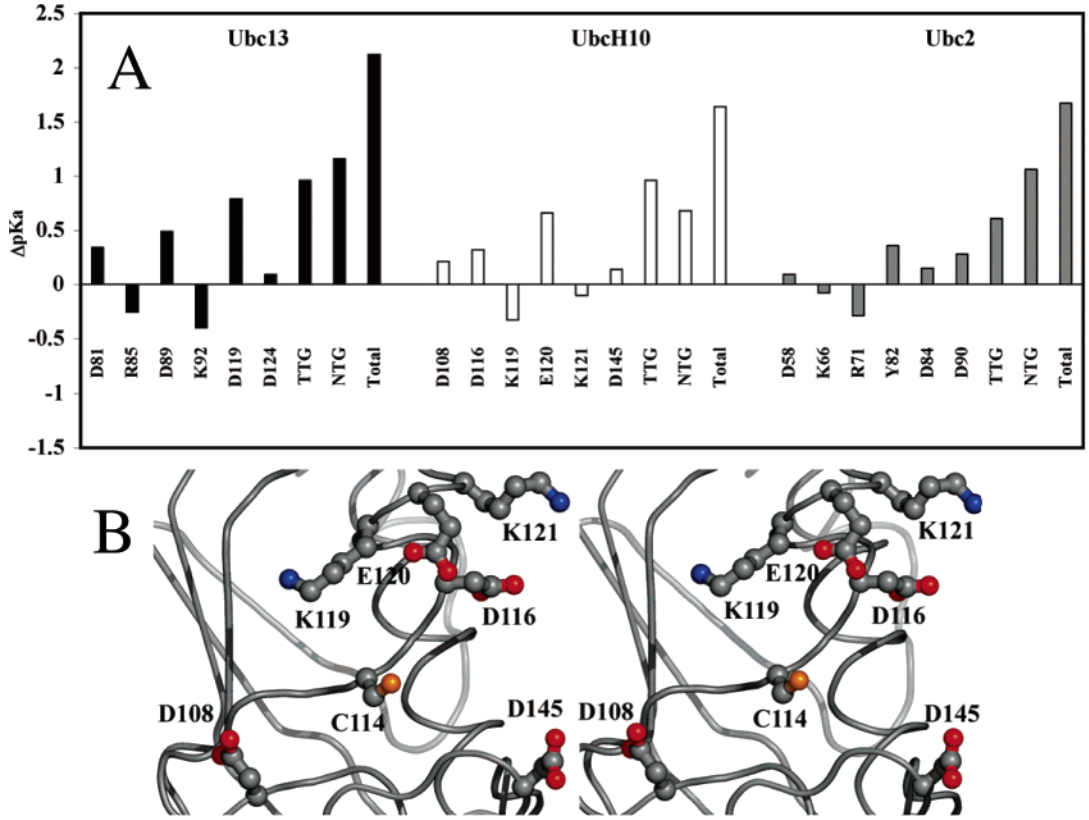

FIGURE 3: Decomposed pK_a values. (A) Ubc13 (black), UbcH10 (white), and Ubc2 (gray). TTG stands for total titratable groups, and NTG stands for nontitratable groups. (B) Zoomed in divergent stereoview of UbcH10 active site geometry showing the most important effectors. Panel B was prepared with PyMol (*20*).

```
UBC10_HUMAN  SLEFPSGYPYNAPTVKFLTPCYHPNVDTQGNICLDILKEKWSALYDVRTILLSIQSLLGEPNIDSPLNTHAA
UBC2_HUMAN   VIDFSEEYPNKPPTVRFLSKMFHPNVYADGSICLDILQNRWSPTYDVSSILTSIQSLLDEPNPNSPANSQAA
UBC13_YEAST  ELYLPDDYPMEAPKVRFLTKIYHPNIDRLGRICLDVLKTNWSPALQIRTVLLSIQALLASPNPNDPLANDVA
UBCC_HUMAN   SLEFPSGYPYNAPTVKFLTPCYHPNVDTQGNICLDILKEKWSALYDVRTILLSIQSLLGEPNIDSPLNTHAA
UBCB_XENLA   SLEFPSGYPYNAPTVKFVTPCFHPNVDSHGNICLDILKDKWSALYDVRTILLSLQSLLGEPNNESPLNPYAA
UBCB_SPISO   TLEFPSDYPYKPPVVKFTTPCWHPNVDQSGNICLDILKENWTASYDVRTILLSLQSLLGEPNNASPLNAQAA
UBCD_SCHPO   SMSFPANYPYSPPTIIFTSPMWHPNVDMSGNICLDILKDKWSAVYNVQTILLSLQSLLGEPNNASPLNAQAA
UBCA_YEAST   SLKFPQNYPFHPPMIKFLSPMWHPNVDKSGNICLDILKEKWSAVYNVETILLSLQSLLGEPNNRSPLNAVAA
UBC3_DROME   ELFLPEDYPMSAPKVRFITKIYHPNIDRLGRICLDVLKDKWSPALQIRTILLSIQALLSAPNPDDPLANDVA
UBCN_HUMAN   ELFLPEEYPMAAPKVRFMTKIYHPNVDKLGRICLDILKDKWSPALQIRTVLLSIQALLSAPNPDDPLANDVA
UBCC_SCHPO   ELFLPDEYPMPPNVRFLTKIYHPNVDKLGRICLSTLKKDWSPALQIRTVLLSIQALMGAPNPDDPLDNDVA
UBCA_HUMAN   TIEFTEEYPNKPPTVRFVSKMFHPNVYADGSICLDILQNRWSPTYDVSSILTSIQSLLDEPNPNSPANSQAA
UBC6_DROME   TIEFTEEYPNKPPTVRFVSKVFHPNVYADGGICLDILQNRWSPTYDVSAILTSIQSLLSDPNPNSPANSTAA
UBC1_CAEEL   SLEFTEEYPNKPPTVKFISKMFHPNVYADGSICLDILQNRWSPTYDVAAILTSIQSLLDEPNPNSPANSLAA
UBC2_CANAL   LLSFDEQYPNKPPQVKFISEMFHPNVYASGELCLDILQNRWSPTYDVSSILTSVQSLLNDPNISSPANVEAA
UBC2_YEAST   LLEFDEEYPNKPPHVKFLSEMFHPNVYANGEICLDILQNRWTPTYDVASILTSIQSLFNDPNPASPANVEAA
UBC2_NEUCR   VMHFEEQYPNKPPSVKFISEMFHPNVYATGELCLDILQNRWSPTYDVAAVLTSIQSLLNDPNTGSPANVEAS
UBC2_SCHPO   VLSFDEQYPNKPPLVKFVSTMFHPNVYANGELCLDILQNRWSPTYDVAAILTSIQSLLNDPNNASPANAEAA
UBC2_MEDSA   SLQFSEDYPNKPPTVRFVSRMFHPNIYADGSICLDILQNQWSPIYDVAAILTSIQSLLCDPNPNSPANSEAA
UBC2_ARATH   SLQFSEDYPNKPPTVRFVSRMFHPNIYADGSICLDILQNQWSPIYDVAAILTSIQSLLCDPNPNSPANSEAA
UBC1_ARATH   SLQFSEDYPNKPPTVRFVSRMFHPNIYADGSICLDILQNQWSPIYDVAAILTSIQSLLCDPNPNSPANSEAA
UBC2_WHEAT   TLQFTEDYPNKPPTVRFVSRMFHPNIYADGSICLDILQNQWSPIYDVAAILTSIQSLLCDPNPNSPANSEAA
UBC3_ARATH   TLHFTEDYPNKPPIVRFVSRMFHPNIYADGSICLDILQNQWSPIYDVAAVLTSIQSLLCDPNPDSPANAEAA
UB5D_RAT     TIDFPTEYPFKPPKVEFTTRIYHPNVNSNGSICLDILRSQWSPALTISKVLLSISSLLCDPNPDDPLVPEIA
UB5B_HUMAN   TIHFPTDYPFKPPKVAFTTRIYHPNINSNGSICLDILRSQWSPALTISKVLLSICSLLCDPNPDDPLVPEIA
```

FIGURE 4: Sequence alignment of residues modulating the pK_a of the active site cysteine residue in E2 proteins. The first three rows give the sequences of the relevant region in the three E2 proteins that were studied. The residues increasing and decreasing the pK_a of the active site cysteine residue are highlighted in green and red, respectively. The active site cysteine residue is highlighted in yellow. Subsequent rows give corresponding sequences in other representative E2 proteins. Inspection of the alignment reveals generally poor conservation of residue position in modulating the cysteine residue pK_a. Sequence alignment performed using BLAST (*14*).

Figure 4 is a sequence alignment of several E2 proteins illustrating the relative sequence location of those residues that are responsible for the elevated pK_a as compared with several other E2 proteins. Considering only the three E2 proteins experimentally tested, we observe that these residues are not strongly conserved. Indeed, relative to the position of the catalytic cysteine residue, only the two residues at positions −6 and +2 are conserved in all three E2 proteins. The remaining residues appear to be relatively scattered, in both sequence space and spatially (Figures 4 and 5). Comparison with other E2 sequences indicates strong sequence conservation for only residues at positions −6 and +2 but not for the other positions. However, in all sequences, there are acidic and basic residues that conceivably could

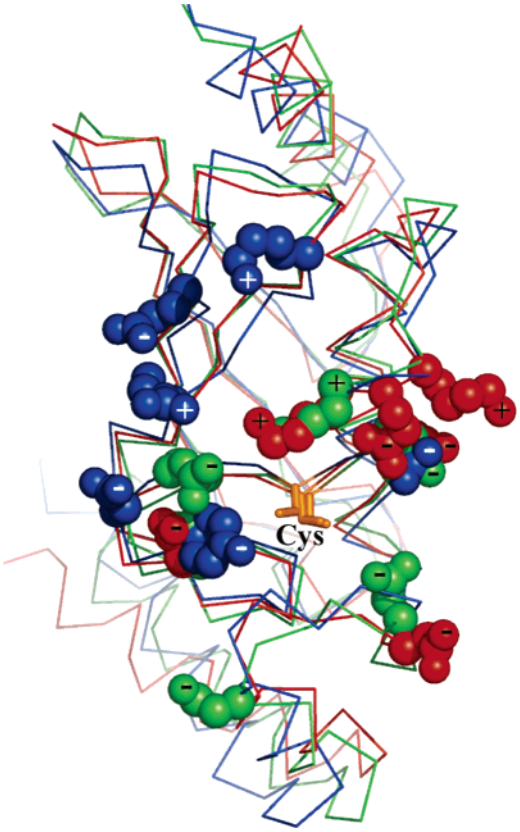

FIGURE 5: Spatial distribution of residues affecting the cysteine pK_a. The structures of UbcH10 (red), Ubc2 (blue), and Ubc13 (green) are superimposed. The active site cysteine side chain is colored yellow and is in stick representation. The residues affecting the cysteine pK_a are shown as van der Waals spheres. Basic residues are marked with a plus sign, and acidic residues (or Tyr) are marked with a minus sign. The spatial locations of these residues generally are not well conserved among the E2 proteins.

modulate the active site pK_a. Thus, the overall electrostatic environment of the active site is likely maintained, but not simply through strict residue conservation. Instead, evolutionary pressure seems to maintain the electrostatic environment through different combinations of residues. The existence of such evolutionary pressure has not been obvious from sequence analysis alone.

Implications for the Mechanism of the Ubiquitination Cascade. The elevated pK_a of the cysteine residue has implications for the transfer of ubiquitin both to and from E2. Since the cysteine residue must be in a thiolate form to accept ubiquitin, the elevated pK_a suggests that E1 and/or ubiquitin association must lower the pK_a of the E2 cysteine residue back toward the pK_a of a model cysteine. The $\Delta\Delta G°$ associated with a ΔpK_a of 2 is on the order of 5RT ($\Delta\Delta G° = 2.3RT\Delta pK_a$) or ~3 kcal/mol. Presumably, the interaction energy associated with the binding of the E1−ubiquitin adduct to E2 is sufficient to shift the pK_a of the active site cysteine to a more reactive value. To this point, this interaction energy has not been characterized. Shaw and coworkers have shown that several arginines of ubiquitin interact with E2 (*18*). Certainly, these charged groups could provide the appropriate electrostatic shielding to promote deprotonation at the catalytic cysteine. Unfortunately, there is no high-resolution structural data for an E1−E2 complex to identify the composition of the binding interface. Schulman and colleagues have determined a cocrystal structure of the Nedd 8 activating enzyme in complex with a peptide fragment of Ubc12. Though it provides a wealth of information, no insight can be gleaned from their structure with regard to the nature of the binding interface between E1 and E2 (*19*). For transfer of ubiquitin, presumably the acidic residues of E2 near the thioester bond would make this bond even more labile, thus facilitating bond cleavage.

Our results have shown that, in isolation, the E2 enzymes are catalytically inactive. This work raises the obvious question of why the pK_a is elevated to such a nonfunctional value. One hypothesis is that this is an evolutionarily conserved control mechanism, which prevents promiscuous reactivity of the E2 proteins with other reactive moieties in the cell. The active cysteine residues of the E2 proteins are highly exposed due to the mechanism of ubiquitination that has evolved. Thus, according to this hypothesis, the cell is able to prevent unwanted reactions with this highly exposed cysteine residue by maintaining it in an electrostatic environment that renders it inactive. The rather surprising findings presented here indicate that the ubiquitin−proteasome system has layers of regulation only now beginning to be understood. We are hopeful the data presented herein will serve as a springboard for further work with a goal of understanding how the ubiquitin−proteasome system actually functions in the context of the cell.

REFERENCES

1. Hershko, A., and Ciechanover, A. (1998) The ubiquitin system, *Annu. Rev. Biochem. 67*, 425−79.
2. Pickart, C. M. (2001) Mechanisms underlying ubiquitination, *Annu. Rev. Biochem. 70*, 503−33.
3. Wu, P. Y., Hanlon, M., Eddins, M., Tsui, C., Rogers, R. S., Jensen, J. P., Matunis, M. J., Weisman, A. M., Wolberger, C. P., and Pickart, C. M. (2003) A conserved catalytic residue in the ubiquitin conjugating enzyme family, *EMBO J. 22*, 5241−50.
4. Lin, Y., Hwang, W. C., and Basavappa, R. (2002) Structural and functional analysis of the human mitotic-specific ubiquitin conjugating enzyme, UbcH10, *J. Biol. Chem. 277*, 21913−21.
5. Aslanidis, C., and de Jong, P. J. (1990) Ligation-idependent cloning of PCR products (LIC-PCR), *Nucleic Acids Res. 18*, 6069−74.
6. Schlegel, B. P., Jez, J. M., and Penning, T. M. (1998) Mutagenesis of 3α-hydroxysteroid dehydrogenase reveals a "push-pull" mechanism for proton transfer in aldo-keto reductases, *Biochemistry 37*, 3538−48.
7. Tajc, S. G., Tolbert, B. S., Basavappa, R., and Miller, B. L. (2004) Direct determination of thiol pK_a by isothermal titration microcalorimetry, *J. Am. Chem. Soc. 126*, 10508−9.
8. Berman, H. M., Westbrook, J., Feng, Z., Gilliland, G., Bhat, T. N., Weissig, H., Shindyalov, I. N., and Bourne, P. E. (2000) The Protein Databank, *Nucleic Acids Res. 28*, 235−42.
9. Vriend, G. (1990) WHAT IF: A molecular modeling and drug design program, *J. Mol. Graphics 8*, 52−6.
10. Nielsen, J. E., and Vriend, G. (2001) Optimizing the hydrogen-bond network in Poisson−Boltzmann equation-based pK_a calculations, *Proteins 43*, 403−12.
11. Nicholls, A., and Honig, B. (1991) A rapid finite difference algorithm, utilizing successive over-relaxation to solve the Poisson−Boltzmann equation, *J. Comput. Chem. 12*, 435−45.
12. Yang, A. S., Gunner, M. R., Sampogna, R., Sharp, K., and Honig, B. (1993) On the calculation of pK_as in proteins, *Proteins 15*, 252−65.
13. Dyson, H. J., Jeng, M. F., Tennant, L. L., Slaby, I., Lindell, M., Cui, D. S., Kuprin, S., and Holmgren, A. (1997) Effects of buried charged groups on cysteine thiol ionization and reactivity in *Escherichia coli* thioredoxin: Structural and functional characterization of mutants of Asp 26 and Lys 57, *Biochemistry 36*, 2622−36.
14. Altschul, S. F., Gish, W., Miller, W., Myers, E. W., and Lipman, D. J. (1990) Basic local alignment search tool, *J. Mol. Biol. 215*, 403−10.

15. Kortemme, T., and Creighton, T. E. (1995) Ionisation of cysteine residues at the termini of model α-helical peptides. Relevance to unusual thiol pK_a values in proteins of the thioredoxin family, *J. Mol. Biol. 253*, 799−812.
16. Gladysheva, T., Liu, J., and Rosen, B. P. (1996) His-8 lowers the pK_a of the essential Cys-12 residue of the ArsC arsenate reductase of plasmid R773 *J. Biol. Chem. 271*, 33256−60.
17. VanDemark, A. P., Hofmann, R. M., Tsui, C., Pickart, C. M., and Wolberger, C. (2001) Molecular insights into polyubiquitin chain assembly: Crystal structure of the Mms2/Ubc13 heterodimer, *Cell 105*, 711−20.
18. Hamilton, K. S., Ellison, M. J., and Shaw, G. S. (2000) Identification of the ubiquitin interfacial residues in a ubiquitin-E2 covalent complex, *J. Biomol. NMR 18*, 319−27.
19. Huang, D. T., Miller, D. W., Mathew, R., Cassell, R., Holton, J. M., Roussel, M. F., and Schulman, B. A. (2004) A unique E1-E2 interaction required for optimal conjugation of the ubiquitin-like protein NEDD8, *Nat. Struct. Mol. Biol. 11*, 927−35.
20. DeLano, W. L. (2003) *PyMol*, DeLano Scientific, South San Francisco, CA (http://www.pymol.org).

BI0514459